光学学报

非对称纠缠相干态损耗信道的传输特性

张笑然[1]，乔晨宇[1]，陈杲乐[1]，王美红[1,2*]，苏晓龙[1,2]

[1]山西大学光电研究所光量子技术与器件全国重点实验室，山西 太原 030006；

[2]极端光学协同创新中心，山西 太原 030006

摘要 非对称纠缠相干态作为连续变量体系中的重要纠缠资源，在提升量子精密测量灵敏度方面具有重要应用。然而，实际信道中的损耗会导致量子态退相干，严重影响其保真度与纠缠特性。本文实验制备了非对称奇、偶纠缠相干态，并验证了不同分束比对纠缠相干态保真度和对数负性的影响。进一步从理论上研究了非对称纠缠相干态在损耗信道中的传输特性，分析了在单信道和双信道方案中非对称纠缠相干态的保真度和对数负性的变化规律。研究发现，在单信道和双信道方案中，随着传输效率的降低，非对称纠缠相干态的保真度和对数负性随之降低。当非对称纠缠相干态的保真度低于0.5时，对数负性依然大于0，即纠缠始终存在，证实了非对称纠缠相干态的纠缠特性在损耗信道中的鲁棒性。该工作为非对称纠缠相干态的参数优化与实际应用提供了依据。

关键词 薛定谔猫态；纠缠相干态；损耗信道；量子精密测量

中图分类号 O436 **文献标志码** A **DOI**：10.3788/AOS260585

1 引 言

量子纠缠态是量子信息中的关键资源之一[1]，在量子计算[2-4]、量子通信[5-10]和量子精密测量[11-13]等领域发挥着不可替代的作用。纠缠相干态是一种重要的连续变量纠缠资源[14-15]，基于纠缠相干态的量子隐形传态方案能够突破经典极限，实现高保真度的量子态传输[15]；此外，纠缠相干态在量子精密测量领域也展现出提升测量精度的潜力[16]。与对称纠缠相干态相比，非对称纠缠相干态在量子传感中具有更高的灵敏度[17]，可作为一种有效的量子资源，为量子精密测量提供更大的量子Fisher信息。在特定参数区间内，非对称纠缠相干态能够突破海森堡极限并展现出更强的抗损耗能力[18]。

然而，在实际传输过程中，信道损耗会引发量子态退相干，导致量子态的保真度与纠缠度衰减[19-20]，从而制约了量子技术的实际性能。近年来，已有研究关注光学猫态在噪声环境中的特性[21]。例如，实验表明，光学猫态的Wigner函数负值区域对损耗极为敏感，但其量子相干性却表现出显著的鲁棒性[22]。此外，信道损耗会降低高斯纠缠态的纠缠度[23-24]，近期理论研究表明，在连续变量纠缠交换过程中引入非高斯操作（如光子减法），能够有效增强交换后纠缠态的纠缠度[25]。上述研究深化了对量子态退相干机制的理解，但针对非对称纠缠相干态在损耗信道中的传输特性，尚缺乏系统性分析。因此，系统研究非对称纠缠相干态在损耗信道中的传输特性，揭示其量子特性的演化规律，对推动其走向实用化至关重要。

本文系统研究了损耗信道中非对称纠缠相干态的传输特性。采用分束器模型模拟损耗信道，分析了不同分束比下制备的非对称纠缠相干态的传输特性，包括单信道与双信道方案中保真度和对数负性的变化规律。结果表明，在单信道和双信道方案中，随着传输效率的降低，非对称奇、偶纠缠相干态的保真度和对数负性均随之下降，且双信道损耗下的衰减速度更快。当保真度低于0.5时，对数负性仍大于0，这意味着纠缠始终存在，表明非对称纠缠相干态的纠缠特性在损耗信道中具有鲁棒性。这些结果为非对称纠缠相干态在实际损耗环境中的参数选择与优化提供了理论依据与设计指导。

2 制备及传输

纠缠相干态可通过光学薛定谔猫态经由分束器分束制备[26]。光学猫态$|\mathrm{cat}\rangle$是幅度相同、相位相反的两个相干态的叠加，表示为

收稿日期：2026-02-02；**修回日期**：2026-03-06；**录用日期**：2026-03-18；**网络首发日期**：2026-04-08

基金项目：“量子通信与量子计算机”国家科技重大专项（2024ZD0302403）、国家自然科学基金（12434015，62275145）、山西省基础研究计划（202403021224001）、山西省“1331工程”重点学科建设经费

通信作者：*wangmh@sxu.edu.cn

$$|\mathrm{cat}\rangle=\frac{1}{\sqrt{N}}\left(|\alpha\rangle+e^{i\theta}|-\alpha\rangle\right) \tag{1}$$

式中：$|\alpha\rangle$为幅度为α的相干态；N为归一化系数，$N=2\left(1+\exp\left(-2|\alpha|^2\right)\cos\theta\right)$。$\theta$为两个相干态之间的相对相位，当$\theta=0$时，该态称为偶猫态$|\mathrm{cat}_+\rangle$；当$\theta=\pi$时，称为奇猫态$|\mathrm{cat}_-\rangle$。如图 1(a)所示，将光学猫态输入透射率为$t$、反射率为$r$的分束器（满足$t+r=1$）进行分束，所制备的纠缠相干态$|\varphi\rangle$可表示为

$$|\varphi\rangle=\frac{1}{\sqrt{N}}\left(|\sqrt{t}\,\alpha\rangle_{\mathrm{a}}|\sqrt{r}\,\alpha\rangle_{\mathrm{b}}+e^{i\theta}|-\sqrt{t}\,\alpha\rangle_{\mathrm{a}}|-\sqrt{r}\,\alpha\rangle_{\mathrm{b}}\right) \tag{2}$$

式中：下标 a 和 b 表示纠缠相干态的两个模式。当$\theta=0$时，该态为偶纠缠相干态$|\varphi_+\rangle$；当$\theta=\pi$时，为奇纠缠相干态$|\varphi_-\rangle$。当$t=r$时，交换两模式后纠缠相干态保持不变，称为对称纠缠相干态；若$t\neq r$，交换两模式后态的形式发生变化，称为非对称纠缠相干态[18]。

考虑图 1(a)所示的损耗信道模型，纠缠相干态的两个模式 a 和 b 分别经传输效率为η_1和η_2的损耗信道发送至 Alice 和 Bob。为分析其传输特性，采用分束器模型模拟信道损耗，即将两模式分别通过传输效率为η_1和η_2的分束器与真空态耦合。随后，在 Alice 和 Bob 端，输出光场分别与本地振荡光在 50∶50 分束器上耦合，进行平衡零拍探测。经损耗信道后的态可表示为

$$|\varphi'_{\pm}\rangle=\frac{1}{\sqrt{N'_{\pm}}}\cdot$$
$$\left(|\sqrt{\eta_1 t}\,\alpha\rangle_{\mathrm{a}'}|\sqrt{\eta_2 r}\,\alpha\rangle_{\mathrm{b}'}|\sqrt{1-\eta_1}\,\sqrt{t}\,\alpha\rangle_{\mathrm{l}_1}|\sqrt{1-\eta_2}\,\sqrt{r}\,\alpha\rangle_{\mathrm{l}_2}\pm|-\sqrt{\eta_1 t}\,\alpha\rangle_{\mathrm{a}'}|-\sqrt{\eta_2 r}\,\alpha\rangle_{\mathrm{b}'}|-\sqrt{1-\eta_1}\,\sqrt{t}\,\alpha\rangle_{\mathrm{l}_1}|-\sqrt{1-\eta_2}\,\sqrt{r}\,\alpha\rangle_{\mathrm{l}_2}\right) \tag{3}$$

式中：$N'_{\pm}$为奇偶纠缠相干态的归一化系数，$N'_{\pm}=2\left(1\pm\exp\left(-2|\alpha|^2\right)\right)$；下标 a′和 b′分别表示经过损耗信道后的模式，下标l_1和l_2分别表示模式 a 和模式 b 与分束器耦合后进入环境的两个损耗模式。若仅有一个模式经过损耗信道（单信道方案），则$\eta_1=1,\eta_2\neq1$或$\eta_1\neq1,\eta_2=1$；若两个模式均经历损耗（双信道方案），则$\eta_1\neq1,\eta_2\neq1$。

为验证纠缠相干态制备方法的可行性，搭建如图 1(b)所示的实验装置，其中 HWP 为半波片、PBS 为偏振分束器、APD 为雪崩光电二极管、PPKTP 为周期性极化磷酸氧钛钾晶体。光纤激光器输出波长 795 nm 的激光（对应铷原子 D1 吸收线），经 HWP 1 和 PBS 1 后分为两束。一束注入光学参量放大器（OPA），另一束经 PBS 2 后进一步分束，其中一路注入倍频腔（SHG）以产生 397.5 nm 蓝紫光，作为 OPA 的泵浦光，另一路用作平衡零拍探测的本地振荡光（LO）。SHG 采用四镜环形腔结构，当基频光注入功率为 50 mW 时，可获得约 25 mW 的 397.5 nm 蓝紫光，转换效率达 50%。该倍频光作为 OPA 的泵浦源，通过参量下转换过程产生压缩真空态。当泵浦光功率为 25 mW 时，OPA 可产生约 −3 dB 的压缩真空态。实验中采用庞德-德雷弗-霍尔（PDH）锁频技术锁定 OPA 腔长，同时将注入光与泵浦光之间的相对相位锁定为 0，从而获得相位压缩态[27]。

OPA 产生的压缩真空态通过一个由 HWP 2 和 PBS 3 组成、透射率为 5% 的分束器，进行减光子操作。透射部分经过由一个滤波片（IF）和两个滤波腔（FC）组成的滤波系统后，由单光子探测器探测所减去

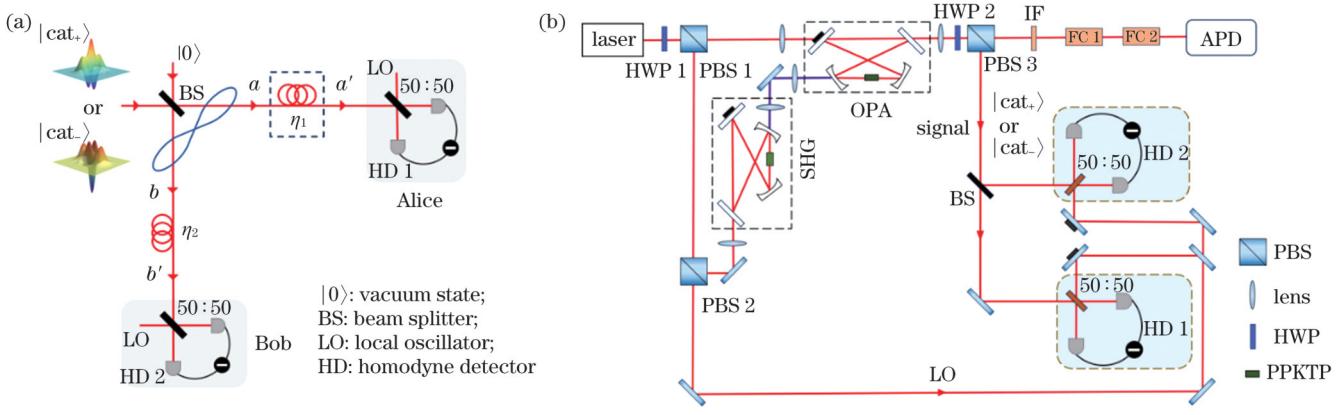

图 1　纠缠相干态的制备与传输示意图。(a)损耗信道中纠缠相干态传输示意图；(b)制备纠缠相干态的实验装置

Fig. 1　Schematic diagrams of preparation and transmission of entangled coherent states. (a) Diagram of transmission of entangled coherent states in lossy channels; (b) experimental setup for preparing entangled coherent states

的单光子。若成功减去一个光子，反射部分对应奇猫态；若未减去光子，则对应偶猫态。制备的光学猫态经透射率为 t 的分束器分束后，透射光和反射光分别与两束本地振荡光在 50∶50 分束器上耦合，进行平衡零拍探测。在平衡零拍探测中，通过压电陶瓷扫描本地振荡光与信号光之间的相对相位，记录不同相位下的光电流，从而获得光场正交分量的概率分布，并采用最大似然估计方法重构纠缠相干态的密度矩阵[28-29]。

为表征损耗信道中非对称纠缠相干态的传输特性，分析其保真度和对数负性的变化。保真度 F 用于度量经损耗信道后纠缠相干态（混合态）与理想纠缠相干态（纯态）的相似程度，定义为 $F=\mathrm{Tr}(\boldsymbol{\rho}'_{\mathrm{ab}}\boldsymbol{\rho}_{\mathrm{ab}})$。其中，$\boldsymbol{\rho}_{\mathrm{ab}}$ 为理想纠缠相干态的密度矩阵，$\boldsymbol{\rho}_{\mathrm{ab}}=\left|\varphi_{\pm}\right\rangle\left\langle\varphi_{\pm}\right|$，$\boldsymbol{\rho}'_{\mathrm{ab}}$ 为经损耗信道后纠缠相干态的密度矩阵。通过对损耗模式 l_1 和 l_2 求迹，得到经损耗信道后纠缠相干态的约化密度矩阵。在单信道方案中（以 $\eta_1=1,\eta_2\neq1$ 为例），经损耗信道后的纠缠相干态密度矩阵可表示为

$$\begin{aligned}\boldsymbol{\rho}'_{\mathrm{ab,\,single\text{-}channel}}=&\mathrm{Tr}\left(\left(\hat{I}_{\mathrm{a}}\otimes\hat{U}_{\mathrm{BS}}^{(\mathrm{b},\mathrm{l}_2)}(\eta_2)\right)\left(\boldsymbol{\rho}_{\mathrm{ab}}\otimes|0\rangle_{\mathrm{l}_2}\langle0|\right)\left(\hat{I}_{\mathrm{a}}\otimes\hat{U}_{\mathrm{BS}}^{(\mathrm{b},\mathrm{l}_2)\dagger}(\eta_2)\right)\right)=\\&\frac{1}{N'_{\pm}}\left(\left|\sqrt{t}\,\alpha,\sqrt{\eta_2 r}\,\alpha\right\rangle\left\langle\sqrt{t}\,\alpha,\sqrt{\eta_2 r}\,\alpha\right|+\left|-\sqrt{t}\,\alpha,-\sqrt{\eta_2 r}\,\alpha\right\rangle\left\langle-\sqrt{t}\,\alpha,-\sqrt{\eta_2 r}\,\alpha\right|\pm\right.\\&\left.\exp\left(-2(1-\eta_2)r|\alpha|^2\right)\left(\left|\sqrt{t}\,\alpha,\sqrt{\eta_2 r}\,\alpha\right\rangle\left\langle-\sqrt{t}\,\alpha,-\sqrt{\eta_2 r}\,\alpha\right|+\left|-\sqrt{t}\,\alpha,-\sqrt{\eta_2 r}\,\alpha\right\rangle\left\langle\sqrt{t}\,\alpha,\sqrt{\eta_2 r}\,\alpha\right|\right)\right)\end{aligned}\tag{4}$$

式中：$\hat{I}_{\mathrm{a}}$ 为模式 a 的单位算符；$|0\rangle_{\mathrm{l}_2}\langle0|$ 为真空态的密度矩阵；$\hat{U}_{\mathrm{BS}}$ 为分束器的酉算符；$\hat{I}_{\mathrm{a}}\otimes\hat{U}_{\mathrm{BS}}^{(\mathrm{b},\mathrm{l}_2)}(\eta_2)$ 表示利用分束器模型将损耗引入模式 b；$\hat{I}_{\mathrm{a}}\otimes\hat{U}_{\mathrm{BS}}^{(\mathrm{b},\mathrm{l}_2)\dagger}(\eta_2)$ 表示 $\hat{I}_{\mathrm{a}}\otimes\hat{U}_{\mathrm{BS}}^{(\mathrm{b},\mathrm{l}_2)}(\eta_2)$ 的厄米共轭。

在双信道方案中，密度矩阵表示为

$$\begin{aligned}\boldsymbol{\rho}'_{\mathrm{ab,\,dual\text{-}channel}}=&\mathrm{Tr}\left(\left(\hat{U}_{\mathrm{BS}}^{(\mathrm{a},\mathrm{l}_1)}(\eta_1)\otimes\hat{U}_{\mathrm{BS}}^{(\mathrm{b},\mathrm{l}_2)}(\eta_2)\right)\left(\boldsymbol{\rho}_{\mathrm{ab}}\otimes|0\rangle_{\mathrm{l}_1}\langle0|\otimes|0\rangle_{\mathrm{l}_2}\langle0|\right)\left(\hat{U}_{\mathrm{BS}}^{(\mathrm{a},\mathrm{l}_1)\dagger}(\eta_1)\otimes\hat{U}_{\mathrm{BS}}^{(\mathrm{b},\mathrm{l}_2)\dagger}(\eta_2)\right)\right)=\\&\frac{1}{N'_{\pm}}\left(\left|\sqrt{\eta_1 t}\,\alpha,\sqrt{\eta_2 r}\,\alpha\right\rangle\left\langle\sqrt{\eta_1 t}\,\alpha,\sqrt{\eta_2 r}\,\alpha\right|+\left|-\sqrt{\eta_1 t}\,\alpha,-\sqrt{\eta_2 r}\,\alpha\right\rangle\left\langle-\sqrt{\eta_1 t}\,\alpha,-\sqrt{\eta_2 r}\,\alpha\right|\pm\right.\\&\left.\exp\left(-2\left((1-\eta_1)t+(1-\eta_2)r\right)|\alpha|^2\right)\left(\left|\sqrt{\eta_1 t}\,\alpha,\sqrt{\eta_2 r}\,\alpha\right\rangle\left\langle-\sqrt{\eta_1 t}\,\alpha,-\sqrt{\eta_2 r}\,\alpha\right|+\left|-\sqrt{\eta_1 t}\,\alpha,-\sqrt{\eta_2 r}\,\alpha\right\rangle\left\langle\sqrt{\eta_1 t}\,\alpha,\sqrt{\eta_2 r}\,\alpha\right|\right)\right)\end{aligned}\tag{5}$$

式中：$|0\rangle_{\mathrm{l}_1}\langle0|$ 为真空态的密度矩阵；$\hat{U}_{\mathrm{BS}}^{(\mathrm{a},\mathrm{l}_1)}(\eta_1)\otimes\hat{U}_{\mathrm{BS}}^{(\mathrm{b},\mathrm{l}_2)}(\eta_2)$ 表示将损耗同时引入模式 a 和 b；$\hat{U}_{\mathrm{BS}}^{(\mathrm{a},\mathrm{l}_1)\dagger}(\eta_1)\otimes\hat{U}_{\mathrm{BS}}^{(\mathrm{b},\mathrm{l}_2)\dagger}(\eta_2)$ 表示 $\hat{U}_{\mathrm{BS}}^{(\mathrm{a},\mathrm{l}_1)}(\eta_1)\otimes\hat{U}_{\mathrm{BS}}^{(\mathrm{b},\mathrm{l}_2)}(\eta_2)$ 的厄米共轭。

以奇纠缠相干态为例，单信道方案中经损耗信道后纠缠相干态的保真度为

$$F_{\mathrm{single\text{-}channel}}=\mathrm{Tr}(\boldsymbol{\rho}'_{\mathrm{ab,\,single\text{-}channel}}\boldsymbol{\rho}_{\mathrm{ab}})=\frac{\cosh\left((1-\eta_2)r|\alpha|^2\right)\sinh^2\left(|\alpha|^2\left(t+r\sqrt{\eta_2}\right)\right)}{\sinh^2\left(|\alpha|^2\right)}\tag{6}$$

双信道方案中经损耗信道后纠缠相干态的保真度为

$$F_{\mathrm{dual\text{-}channel}}=\mathrm{Tr}(\boldsymbol{\rho}'_{\mathrm{ab,\,dual\text{-}channel}}\boldsymbol{\rho}_{\mathrm{ab}})=\frac{\cosh\left(\left((1-\eta_1)t+(1-\eta_2)r\right)|\alpha|^2\right)\sinh^2\left(|\alpha|^2\left(t\sqrt{\eta_1}+r\sqrt{\eta_2}\right)\right)}{\sinh^2\left(|\alpha|\right)^2}\tag{7}$$

为量化量子态的纠缠程度，采用对数负性判据 $E_{\mathrm{N}}(\boldsymbol{\rho})=\log_2\left\|\boldsymbol{\rho}^{\mathrm{T_A}}\right\|_1$ 进行度量[30-31]，该判据可在 Fock 态基矢下计算。其中，$\boldsymbol{\rho}^{\mathrm{T_A}}$ 是密度矩阵 $\boldsymbol{\rho}$ 的部分转置，迹范数表示为 $\left\|\boldsymbol{\rho}^{\mathrm{T_A}}\right\|_1=2N(\boldsymbol{\rho})+1$，$N(\boldsymbol{\rho})$ 为所有负特征值的绝对值之和。当 $E_{\mathrm{N}}(\boldsymbol{\rho})>0$ 时，表明量子态存在纠缠。对于两体系统，$E_{\mathrm{N}}(\boldsymbol{\rho})$ 越大，量子态的纠缠程度越高[31]。

3 结果分析

理想的纠缠相干态需在无限维 Fock 空间中描述，但在实际计算中通常需将希尔伯特空间截断至有限维度进行近似处理[32]。随着输入猫态幅度的增大，纠缠相干态的高光子数项增多。当截断维度为 10 且 $\alpha=\sqrt{2}$ 时，光子数为 9 的概率约为 10^{-4}，截断误差可忽略；而当 $\alpha>\sqrt{2}$ 时，高光子数项进一步增加，截断误差不可忽略。为合理选择截断维度并准确表征纠缠相干态的特性，在截断维度为 10（即最大光子数为 9）的条件下，分析了奇、偶纠缠相干态（以 $t=1/3$ 和 $t=1/9$ 为例）相对于理想纠缠相干态的保真度随猫态幅度 α 的变化，如图 2 所示。无论 $t=1/3$ 还是 $t=1/9$，当 $\alpha<\sqrt{2}$ 时，纠缠相干态的保真度均接近 1；而当 $\alpha>\sqrt{2}$ 时，保真度随 α 增大而下降。以上结果表明，在截断维度为 10 且猫态幅度不超过 $\sqrt{2}$ 的条件下，该截断方案能有效维持较高保真度，通过分束器对光学猫态进行分束的方法在该参数范围内能够高保真地制备纠缠相干态。

为研究不同透射率对纠缠相干态特性的影响，首

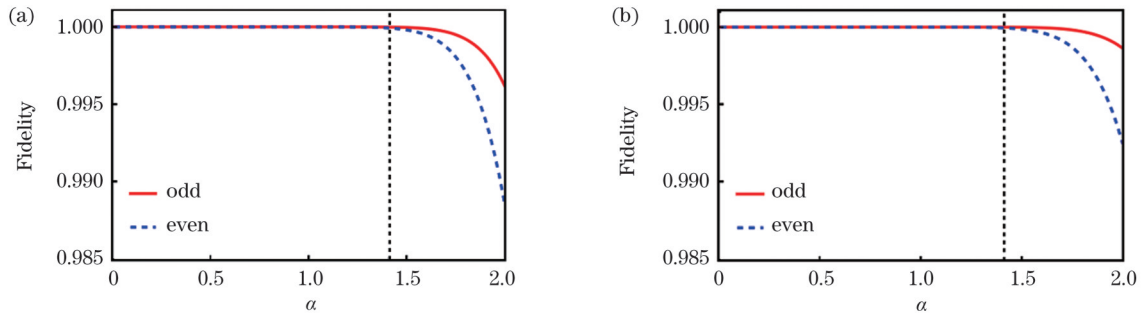

图 2　截断维度为 10 时，奇、偶纠缠相干态的保真度随 α 的变化曲线。(a) $t=1/3$；(b) $t=1/9$

Fig. 2　Fidelity of the odd and even entangled coherent states as functions of α with a truncation dimension of 10. (a) $t=1/3$; (b) $t=1/9$

先在无损耗信道条件下，分析了奇、偶纠缠相干态的保真度和对数负性随分束器透射率 t 的变化，结果如图 3 所示。可以看到，随着透射率的增大，奇、偶纠缠相干态的保真度提高，纠缠度增加；当 $t=1/2$ 时，保真度和纠缠度均达到最大值，表明系统处于最大纠缠态；当透射率超过 1/2 后，保真度和纠缠度随之下降。

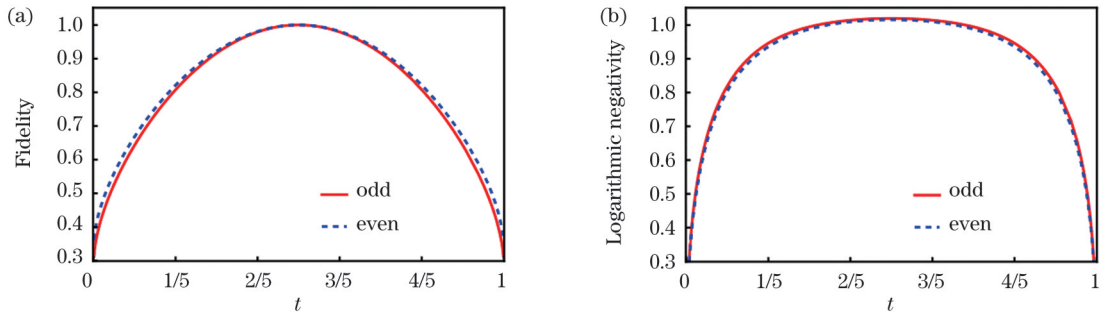

图 3　无损耗信道条件下，奇、偶纠缠相干态的保真度和对数负性随 t 的变化曲线。(a)保真度；(b)对数负性

Fig. 3　Fidelity and logarithmic negativity of the odd and even entangled coherent states as functions of t under lossless channel conditions. (a) Fidelity; (b) logarithmic negativity

通过改变透射率 t，实验制备了非对称奇、偶纠缠相干态，并获得了保真度和对数负性随 t 的变化，实验结果如图 4 所示，图中曲线为理论结果，红色圆点和蓝色三角分别代表奇、偶纠缠相干态的实验数据。实验制备的奇纠缠相干态在 t 为 1/4、1/3、1/2、2/3、3/4 时的保真度分别为 0.60±0.01、0.62±0.02、0.65±0.02、0.61±0.02、0.61±0.01，对数负性分别为 0.61±0.03、0.64±0.02、0.66±0.04、0.64±0.02、0.62±0.03；实验制备的偶纠缠相干态在相同 t 下的保真度分别为 0.91±0.03、0.93±0.01、0.95±0.02、0.93±0.01、0.91±0.03，对数负性分别为 0.35±0.03、0.35±0.02、0.39±0.02、0.35±0.03、0.36±0.02。非零的对数负性证实了奇、偶纠缠相干态的成功制备。随着透射率增大，奇、偶纠缠相干态的保真度和纠缠度均先升高后降低，在 $t=1/2$ 时达到最大值，变化规律与图 3 所示的分析结果一致，验证了该制备方法的可行性。图 4 中的误差棒主要来源于制备态的模式纯度、OPA 腔中注入光与泵浦光相对相位锁定后的相位抖动、光学元件的非理想透射率，以及单光子探测器的探测效率和暗计数等因素。

图 5 展示了单信道方案（$\eta_1=1$，$\eta_2\neq1$）中，以 $t=$

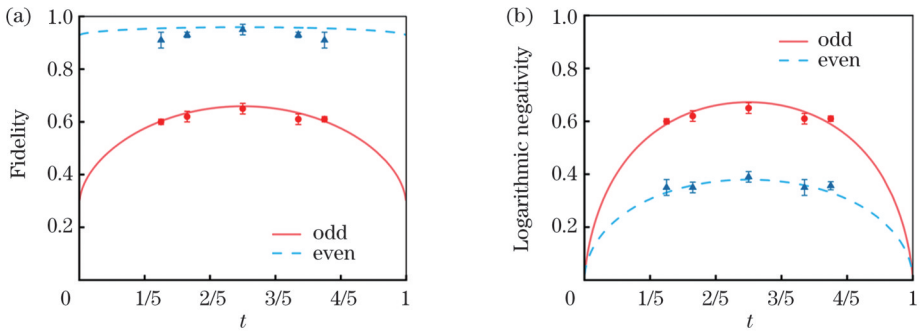

图 4　实验制备的奇、偶纠缠相干态的保真度和对数负性随 t 的变化曲线。(a)保真度；(b)对数负性

Fig. 4　Experimental fidelity and logarithmic negativity of the odd and even entangled coherent states as functions of t. (a) Fidelity; (b) logarithmic negativity

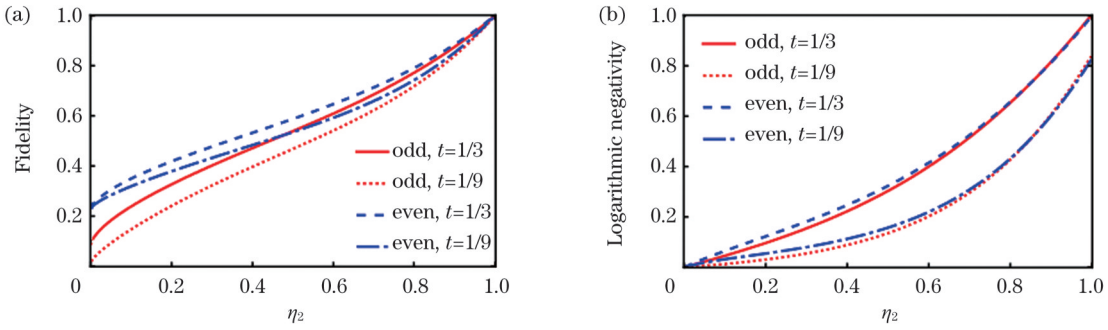

图5　单信道方案中非对称奇、偶纠缠相干态的保真度和对数负性随η_2的变化曲线。(a)保真度;(b)对数负性

Fig. 5　Fidelity and logarithmic negativity of the odd and even asymmetric entangled coherent states as functions of η_2 in the single-channel scheme. (a) Fidelity; (b) logarithmic negativity

1/3和$t=1/9$为例的非对称奇、偶纠缠相干态的保真度和对数负性随传输效率η_2的变化曲线。由图可知,随着η_2的增加,奇、偶纠缠相干态的保真度和对数负性均上升。无论是奇纠缠相干态还是偶纠缠相干态,在不同的透射率下,当保真度低于0.5时,对数负性依然大于0,即纠缠始终存在,表明非对称纠缠相干态的纠缠特性在损耗信道中具有鲁棒性。偶纠缠相干态在整个传输效率范围内均表现出优势,相同透射率下其保真度和对数负性始终高于对应的奇纠缠相干态,表明偶纠缠相干态对损耗具有更强的鲁棒性。这主要是由于偶纠缠相干态包含偶数光子数成分,损耗过程会使其逐步衰减至稳定的真空态,退相干速度较慢;而奇纠缠相干态仅包含奇数光子数成分,更易受损耗影响,退相干速度更快。因此,在相同损耗条件下,偶纠缠相干态的保真度和纠缠度始终高于奇纠缠相干态,表现出更强的鲁棒性。

在双信道方案($\eta_1\neq1,\eta_2\neq1$)中,通过$t=1/3$和$t=1/9$的分束器制备的非对称奇、偶纠缠相干态的保真度和对数负性随传输效率η_1和η_2的变化关系如图6所示。由图可知,随着η_1和η_2的增加,奇、偶纠缠相干

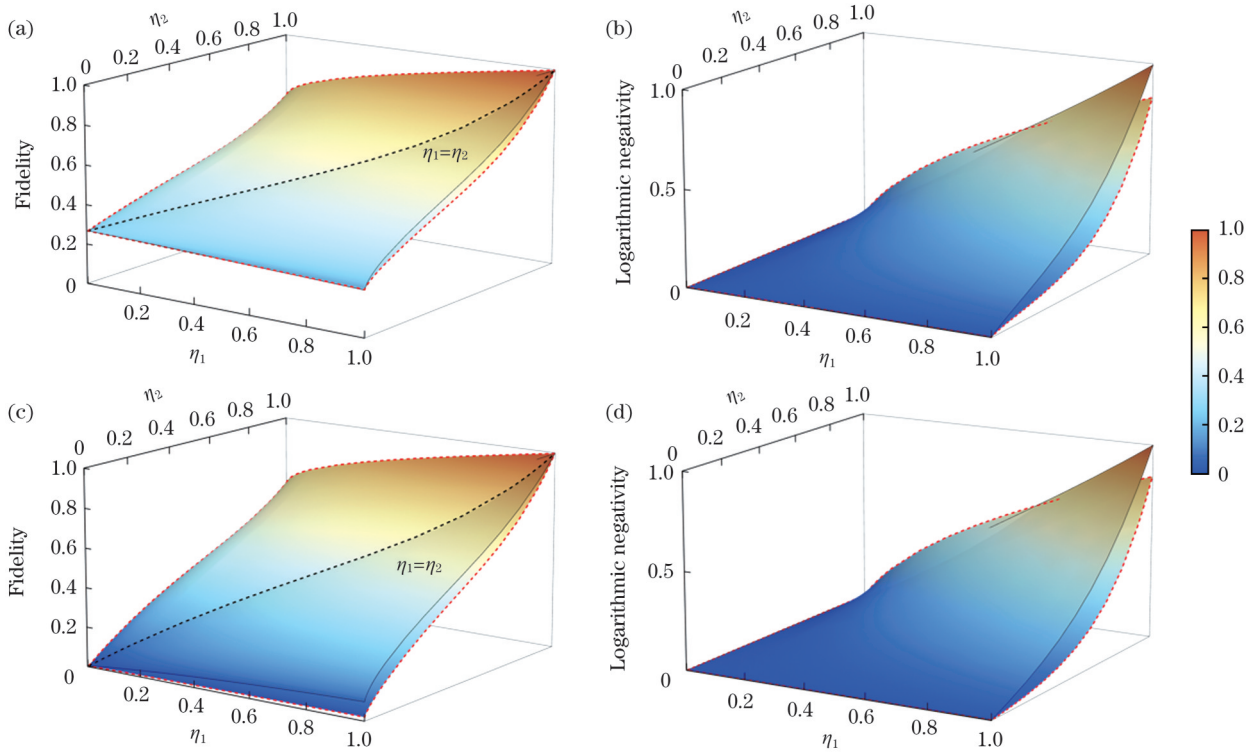

图6　双信道方案中非对称奇、偶纠缠相干态的保真度与对数负性随η_1和η_2的变化关系。(a)偶纠缠相干态保真度;(b)偶纠缠相干态对数负性;(c)奇纠缠相干态保真度;(d)奇纠缠相干态对数负性

Fig. 6　Fidelity and logarithmic negativity of the odd and even asymmetric entangled coherent states as functions of η_1 and η_2 in the dual-channel scheme. (a) Fidelity of even entangled coherent states; (b) logarithmic negativity of even entangled coherent states; (c) fidelity of odd entangled coherent states; (d) logarithmic negativity of odd entangled coherent states

态的保真度和对数负性均上升。当$\eta_1=\eta_2$时(黑色虚线),两种透射率下制备的纠缠相干态保真度相等;当$\eta_1>\eta_2$时,$t=1/3$制备的纠缠相干态(黑色实线边界曲面)的保真度始终高于$t=1/9$制备的纠缠相干态(红色虚线边界曲面);当$\eta_1<\eta_2$时,前者保真度低于后者。结果表明,在非对称损耗($\eta_1\neq\eta_2$)下,不同透射率制备的非对称奇、偶纠缠相干态的保真度衰减速度不同。当保真度低于0.5时,对数负性始终大于0,即纠缠始终存在,证明了双信道方案中非对称奇、偶纠缠相干态量子纠缠的鲁棒性。对比单信道与双信道方案可以发现,双信道方案中非对称纠缠相干态的保真度和对数负性衰减速率更快,但量子纠缠依然具有鲁棒性。

4 结 论

本文研究了分束器分束比对奇、偶纠缠相干态保真度和对数负性的影响,实验制备了不同对称程度的奇、偶纠缠相干态,并验证了制备方法的可行性。进一步从理论上研究了损耗信道中非对称纠缠相干态的传输特性,分析了单信道与双信道方案中非对称纠缠相干态保真度与对数负性的变化规律。结果表明,在单信道和双信道方案中,随着传输效率的降低,非对称奇、偶纠缠相干态的保真度和对数负性均降低,且双信道方案中的衰减速度更快。当存在损耗时,尽管非对称纠缠相干态的保真度会低于0.5,但对数负性始终大于0,即纠缠始终存在,这表明非对称纠缠相干态的纠缠特性在损耗信道中具有鲁棒性。这些结果为纠缠相干态在量子信息处理中的应用提供了重要指导。

参 考 文 献

[1] Andersen U L, Neergaard-Nielsen J S, van Loock P, et al. Hybrid discrete- and continuous-variable quantum information[J]. Nature Physics, 2015, 11(9): 713-719.

[2] Shor P W. Polynomial-time algorithms for prime factorization and discrete logarithms on a quantum computer[J]. SIAM Review, 1999, 41(2): 303-332.

[3] Menicucci N C, van Loock P, Gu M L, et al. Universal quantum computation with continuous-variable cluster states[J]. Physical Review Letters, 2006, 97(11): 110501.

[4] Hao S H, Deng X W, Liu Y, et al. Quantum computation and error correction based on continuous variable cluster states[J]. Chinese Physics B, 2021, 30(6): 060312.

[5] Furusawa A, Sørensen J L, Braunstein S L, et al. Unconditional quantum teleportation[J]. Science, 1998, 282(5389): 706-709.

[6] van Loock P, Braunstein S L. Multipartite entanglement for continuous variables: a quantum teleportation network[J]. Physical Review Letters, 2000, 84(15): 3482-3485.

[7] Ren S Y, Han D M, Wang M H, et al. Continuous variable quantum teleportation and remote state preparation between two space-separated local networks[J]. Science China Information Sciences, 2024, 67(4): 142502.

[8] Jing J T, Zhang J, Yan Y, et al. Experimental demonstration of tripartite entanglement and controlled dense coding for continuous variables[J]. Physical Review Letters, 2003, 90(16): 167903.

[9] Guo Y, Liu B H, Li C F, et al. Advances in quantum dense coding[J]. Advanced Quantum Technologies, 2019, 2(5/6): 1900011.

[10] Chen Y X, Liu S S, Lou Y B, et al. Orbital angular momentum multiplexed quantum dense coding[J]. Physical Review Letters, 2021, 127(9): 093601.

[11] Giovannetti V, Lloyd S, Maccone L. Advances in quantum metrology[J]. Nature Photonics, 2011, 5(4): 222-229.

[12] Pezzé L, Smerzi A. Ultrasensitive two-mode interferometry with single-mode number squeezing[J]. Physical Review Letters, 2013, 110(16): 163604.

[13] Hao S H, Shi H W, Gagatsos C N, et al. Demonstration of entanglement-enhanced covert sensing[J]. Physical Review Letters, 2022, 129(1): 010501.

[14] Sanders B C. Review of entangled coherent states[J]. Journal of Physics A: Mathematical and Theoretical, 2012, 45(24): 244002.

[15] van Enk S J, Hirota O. Entangled coherent states: teleportation and decoherence[J]. Physical Review A, 2001, 64(2): 022313.

[16] Joo J, Munro W J, Spiller T P. Quantum metrology with entangled coherent states[J]. Physical Review Letters, 2011, 107(8): 083601.

[17] Park C Y, Jeong H. Bell-inequality tests using asymmetric entangled coherent states in asymmetric lossy environments[J]. Physical Review A, 2015, 91(4): 042328.

[18] Chen X T, Zhang R, Lu W J, et al. Asymmetry-enhanced phase sensing via asymmetric entangled coherent states[J]. Physical Review A, 2024, 109(4): 042609.

[19] le Jeannic H, Cavaillès A, Huang K, et al. Slowing quantum decoherence by squeezing in phase space[J]. Physical Review Letters, 2018, 120(7): 073603.

[20] Serafini A, de Siena S, Illuminati F, et al. Minimum decoherence cat-like states in Gaussian noisy channels[J]. Journal of Optics B: Quantum and Semiclassical Optics, 2004, 6(6): S591-S596.

[21] Xu F Y, Zhang M, Wang M H, et al. Quantifying quantum coherence of optical cat states in a noisy channel[J]. Optics Continuum, 2025, 4(7): 1554-1562.

[22] Zhang M, Kang H J, Wang M H, et al. Quantifying quantum coherence of optical cat states[J]. Photonics Research, 2021, 9(5): 887-892.

[23] Deng X W, Liu Y, Wang M H, et al. Sudden death and revival of Gaussian Einstein-Podolsky-Rosen steering in noisy channels[J]. npj Quantum Information, 2021, 7: 65.

[24] Liu Y, Zheng K M, Kang H J, et al. Distillation of Gaussian Einstein-Podolsky-Rosen steering with noiseless linear amplification[J]. npj Quantum Information, 2022, 8: 38.

[25] Wang N, Wang M H, Su X L. Continuous-variable entanglement swapping with photon subtraction[J]. Physical Review A, 2024, 110(1): 012416.

[26] Ourjoumtsev A, Ferreyrol F, Tualle-Brouri R, et al. Preparation of non-local superpositions of quasi-classical light states[J]. Nature Physics, 2009, 5(3): 189-192.
[27] Xu F Y, Wang M H, Qiao C Y, et al. Hybrid entanglement carrying orbital angular momentum[J]. Science Bulletin, 2025, 70(6): 876-881.
[28] Qiao C Y, Xu F Y, Wang M H, et al. Experimental preparation of optical cat states carrying orbital angular momentum[J]. Laser & Photonics Reviews, 2024, 18(12): 2400174.
[29] Wang M H, Zhang M, Qin Z Z, et al. Experimental preparation and manipulation of squeezed cat states via an all-optical in-line squeezer[J]. Laser & Photonics Reviews, 2022, 16(12): 2200336.
[30] Vidal G, Werner R F. Computable measure of entanglement[J]. Physical Review A, 2002, 65(3): 032314.
[31] Plenio M B. Logarithmic negativity: a full entanglement monotone that is not convex[J]. Physical Review Letters, 2005, 95(9): 090503.
[32] Mogilevtsev D, Řeháček J, Hradil Z. Objective approach to biased tomography schemes[J]. Physical Review A, 2007, 75(1): 012112.

Transmission Characteristics of Asymmetric Entangled Coherent States in Lossy Channels

Zhang Xiaoran[1], Qiao Chenyu[1], Chen Gaole[1], Wang Meihong[1,2*], Su Xiaolong[1,2]

[1]*State Key Laboratory of Quantum Optics Technologies and Devices, Institute of Opto-Electronics, Shanxi University, Taiyuan* 030006, *Shanxi, China*;

[2]*Collaborative Innovation Center of Extreme Optics, Taiyuan* 030006, *Shanxi, China*

Abstract

Objective As an entanglement resource in continuous-variable systems, asymmetric entangled coherent states find important applications in enhancing the sensitivity of quantum precision measurements. However, in practical transmission processes, channel losses lead to the decoherence of quantum states, resulting in the degradation of their fidelity and entanglement, which limits the practical performance of quantum technologies. Although the properties of optical cat states in lossy channels have been investigated, a systematic analysis of the transmission characteristics of asymmetric entangled coherent states in lossy channels is still lacking. Therefore, toward practical applications, it is important to investigate the transmission characteristics of asymmetric entangled coherent states in lossy channels.

Methods To prepare entangled coherent states, optical Schrödinger cat states are split through a beam splitter (BS). To verify the feasibility of this preparation method, asymmetric odd and even entangled coherent states were experimentally prepared. The transmission characteristics of asymmetric entangled coherent states prepared with different splitting ratios were analyzed. The lossy channel was modeled using a BS model: the two modes of the entangled coherent state were coupled with vacuum states via two BSs of transmission efficiencies η_1 and η_2, respectively, to simulate the channel losses. The transmission characteristics of fidelity and logarithmic negativity in both single-channel (only one mode undergoes the lossy channel) and dual-channel (both modes undergo the lossy channel) schemes were analyzed.

Results and Discussions Under lossless channel conditions, the fidelity and logarithmic negativity of odd and even entangled coherent states as functions of the BS transmittance t were analyzed. As the transmittance increased, the fidelity and logarithmic negativity of both odd and even entangled coherent states increased. When the transmittance reached 1/2, the fidelity and logarithmic negativity attained their maximum, indicating that the system was in a maximally entangled state. When the transmittance exceeded 1/2, both fidelity and logarithmic negativity decreased with increasing transmittance.

By changing the transmittance of the BS, asymmetric odd and even entangled coherent states were experimentally prepared, and the dependence of the fidelity and logarithmic negativity of these states on the transmittance was verified. The nonzero logarithmic negativity confirmed the successful preparation of the odd and even entangled coherent states. As the transmittance increased, the fidelity and logarithmic negativity of both odd and even entangled coherent states first increased and then decreased, reaching their maximum at $t=1/2$. This trend is consistent with the theoretical analysis, verifying the feasibility of the preparation method used in this work.

The dependence of fidelity and logarithmic negativity of asymmetric odd and even entangled coherent states (taking $t=1/3$ and $t=1/9$ as examples) on the transmission efficiency in the single-channel ($\eta_1=1$, $\eta_2\neq1$) and dual-channel ($\eta_1\neq1$, $\eta_2\neq1$) schemes was analyzed. As the transmission efficiency increased, the fidelity and logarithmic negativity of both odd and even states increased.

Regardless of the splitting ratio, the logarithmic negativity remained greater than 0 even when the fidelity was lower than 0.5, confirming the robustness of the entanglement of asymmetric entangled coherent states against channel loss. Over the entire range of transmission efficiencies, the even entangled coherent states consistently exhibited higher fidelity and logarithmic negativity than the odd entangled coherent states, indicating that the even states possess stronger robustness against channel loss. In the dual-channel schemes, under asymmetric loss conditions ($\eta_1 \neq \eta_2$), the decay rates of fidelity differed for asymmetric entangled coherent states prepared with different splitting ratios. Comparing the single- and dual-channel schemes, the fidelity and logarithmic negativity decreased more rapidly in the dual-channel scheme, yet quantum entanglement remained robust against channel loss.

The transmission characteristics of asymmetric entangled coherent states in lossy channels are investigated within a finite-dimensional truncated approximation. Theoretical analysis indicates that increasing the amplitude of the input cat state would further enhance the sensitivity of asymmetric entangled coherent states in quantum precision measurements, but a higher truncation dimension would be required. Therefore, studying the transmission characteristics of large-amplitude asymmetric entangled coherent states in lossy channels represents a valuable direction for future research. In practical applications, various additional noises are introduced by channels. For example, the dominant noise in atmospheric channels arises from atmospheric turbulence, while fiber channels may be affected by nonlinear scattering. Hence, investigating the transmission characteristics of asymmetric entangled coherent states in noisy channels by incorporating specific noise models is another worthwhile direction for further exploration.

Conclusions In this study, asymmetric odd and even entangled coherent states were experimentally prepared, and the dependence of the fidelity and logarithmic negativity of the entangled coherent states on different beam-splitting ratios were experimentally verified. Furthermore, the transmission characteristics of asymmetric entangled coherent states in lossy channels were investigated, and the effect of loss on the fidelity and logarithmic negativity in both single- and dual-channel schemes was analyzed. The fidelity and logarithmic negativity of asymmetric entangled coherent states decrease with decreasing transmission efficiency in both schemes. The logarithmic negativity remains greater than 0 even when the fidelity is lower than 0.5, confirming the robustness of the entanglement of asymmetric entangled coherent states against channel loss. These results provide a theoretical basis for parameter optimization and applications of asymmetric entangled coherent states.

Key words Schrödinger cat state; entangled coherent state; lossy channel; quantum precision measurement